

A fracture model with variable range of interaction

Raul Cruz Hidalgo¹, Yamir Moreno², Ferenc Kun³ and Hans J. Herrmann¹

¹ *ICA1, University of Stuttgart, Pfaffenwaldring 27, 70569 Stuttgart, Germany.*

² *The Abdus Salam International Centre for Theoretical Physics,
Condensed Matter Group, P.O. Box 586, Trieste, I-34014, Italy.*

³ *Department of Theoretical Physics, University of Debrecen, P. O. Box: 5, H-4010 Debrecen, Hungary.*
(November 7, 2018)

We introduce a fiber bundle model where the interaction among fibers is modeled by an adjustable stress-transfer function which can interpolate between the two limiting cases of load redistribution, the global and the local load sharing schemes. By varying the range of interaction several features of the model are numerically studied and a crossover from mean field to short range behavior is obtained. The properties of the two regimes and the emergence of the crossover in between are explored by numerically studying the dependence of the ultimate strength of the material on the system size, the distribution of avalanches of breakings, and of the cluster sizes of broken fibers. Finally, we analyze the moments of the cluster size distributions to accurately determine the value at which the crossover is observed.

I. INTRODUCTION

Fracture processes have attracted the attention of the scientific community since many years. Processes involving heterogeneous systems, for which a definite and complete physical description has not been found despite the many partial successes of the last decades, are of special theoretical and practical interest. [1–3]. In particular, the latest developments of statistical mechanics have led to a deeper understanding of breakdown phenomena in heterogeneous systems, but some fundamental questions remain unsolved. The difficulties arise because in modeling fracture of heterogeneous materials, one has to deal with systems formed by many interacting constituents, each one having different statistical properties related to some breaking characteristics of the material, distributed randomly in space and/or time [1,2]. So, the complete analytical solution is in almost all cases prohibitive and one has to solve the problem by means of numerical simulations or to study simplified models which can be analytically tractable (at least in some limits) in order to gain physical insights that guide our understanding to more complex models.

The major challenge in dealing with fracture problems is to combine the statistical evolution of damage across the entire macroscopic system and the associated stress redistributions to accurately predict the point of final rupture of the material. In doing this linkage, one has to take care in order not to make major simplifications particularly in the redistribution rule, where a great deal of the physics of the problem is hidden. A very important class of approaches to the fracture problem are the well-known Fiber Bundle Models (FBM), which were introduced long time ago by Daniels [4] and Coleman [5] and have been the subject of intense research during the last several years [6–20]. FBM's are constructed so that

a set of fibers is arranged in parallel each one having a statistically distributed strength. The specimen is loaded parallel to the fiber direction and the fibers break if the load acting on them exceeds their threshold value. Once the fibers begin to fail one can choose among several load transfer rules. The simplest case is to assume global load sharing (GLS) which means that after each fiber failure, its load is equally redistributed among all the intact fibers remaining in the set. This model, known as global fiber bundle model, is a mean field approximation where long range interactions among the elements of the system are assumed and can be solved analytically [14,18]. At the other extreme, one finds the local load sharing (LLS) fiber bundle model where the load borne by failing elements is transferred to their nearest neighbors. This case represents short range interactions among the fibers. Other schemes have been proposed with a relative success in describing rupture processes at large scale like earthquakes [21].

Despite their simplicity, FBM are very important because they capture most of the main aspects of material damage and breakdown. They have provided a deeper understanding of fracture processes and have served as a starting point for more complex models of fiber reinforced composites and other micro-mechanical models [22–24]. However, stress redistribution in actual heterogeneous materials should fall somewhere in between LLS and GLS since there is an important fraction of stress redistributed to other intact elements not localized in the neighborhood of the failed ones, nevertheless maintaining stress concentrations around the broken fibers. With this aim, several studies have been carried out during the last two decades and Monte Carlo simulations have been used to numerically study the distribution of composite strengths in 2D and 3D for different fiber arrangements [16,25–29]. Nevertheless, in order to obtain reliable con-

clusions the number of fibers forming the system has to be very large which makes the numerical problem, in many cases, too time consuming as to perform the study in a reasonable amount of time.

In this paper, we introduce a fiber bundle model where the interaction among fibers is modeled by an adjustable stress-transfer function, which interpolates between the two limiting cases of load redistribution, the global and the local load sharing schemes. By varying the effective range of interaction one observes a crossover from mean field to short range behavior. To explore the properties of the two regimes and the emergence of the crossover in between, a comprehensive numerical study of the model is performed. We study the dependence of the ultimate strength of the material on the system size and found that the system has only one nonzero critical load in the thermodynamic limit. When no critical point exists, the ultimate strength of the material goes to zero exactly as in local load sharing models as $\sim \frac{1}{\ln(N)}$, with increasing system size N . We also study the distribution of avalanches of fiber breaks, and that of the cluster sizes of broken fibers for the two distinct regimes and perform a moment analysis to accurately determine the crossover value.

The rest of the paper is organized as follows. The next section is devoted to present the model and the way in which numerical simulations are carried out. The results obtained are presented and analyzed in Section III. The final section is devoted to discussions and to state our conclusions.

II. THE MODEL

The fracture of heterogeneous systems is characterized by the highly localized concentration of stresses at the crack tips that makes possible the nucleation of new cracks at these regions such that the actual crack grows leading to the final collapse of the system. In elastic materials, the stress redistribution follows a power law,

$$\sigma_{add} \sim r^{-\gamma}, \quad (1)$$

where σ_{add} is the stress increase on a material element at a distance r from the crack tip. The above general relation covers the cases of global and local load sharing, widely used in fiber bundle models of fracture, as the limiting cases $\gamma \rightarrow 0$, and $\gamma \rightarrow \infty$, respectively.

Motivated by the above result of fracture mechanics we introduce a fiber bundle model where the load sharing rule takes the form of Eq. (1). Suppose a set of N parallel fibers each one having statistically distributed strength taken from a probability distribution function P and identified by an integer i , $1 \leq i \leq N$. In materials science, the Weibull distribution has been proved to be a good empirical statistical distribution for representing fiber strength,

$$P(\sigma) = 1 - e^{-\left(\frac{\sigma}{\sigma_0}\right)^\rho},$$

where ρ is the so-called Weibull index, which controls the degree of threshold disorder in the system (the bigger the Weibull index, the narrower the range of threshold values), and σ_0 is a reference load which acts as unity. Thus, to each fiber i a random threshold value $\sigma_{i_{th}}$ is assigned. The system is driven by increasing quasistatically the load on it, which is performed by locating the fiber which minimizes $\sigma_i - \sigma_{i_{th}}$ and adding this amount of load to all the intact fibers in the system. This provokes the failure of at least one fiber which transfers its load to the surviving elements of the set. This may provoke other fractures in the system which in turn induce tertiary ruptures and so on until the system fails or reaches an equilibrium state where the load on the intact fibers is lower than their individual strengths. In this later case, the slow external driving is applied again and the process is repeated up to the macroscopic failure of the material. The number of broken fibers between two successive external drivings is the size of an avalanche s , and the number of parallel updatings of the lattice during an avalanche is called its lifetime T .

We now focus on the load transfer process following fiber failures. We suppose that, in general, all intact fibers have a nonzero probability of being affected by the ongoing failure event, and that the additional load received by an intact fiber i depends on its distance r_{ij} from fiber j which has just been broken. Furthermore, elastic interaction is assumed between fibers such that the load received by a fiber follows the power law form of Eq. (1). Hence, in our discrete model the stress-transfer function $F(r_{ij}, \gamma)$ takes the form

$$F(r_{ij}, d) = Z r_{ij}^{-\gamma}, \quad (2)$$

where γ is our adjustable parameter, Z is given by the normalization condition $Z = \left(\sum_{i \in I} r_{ij}^{-\gamma}\right)^{-1}$ (the sum runs over the set I of all intact elements) and r_{ij} is the distance of fiber i to the rupture point (x_j, y_j) , *i.e.*, $r_{ij} = \sqrt{(x_i - x_j)^2 + (y_i - y_j)^2}$ in 2D. Periodic boundary conditions are assumed so that the largest r value is $R_{max} = \frac{\sqrt{2}(L-1)}{2}$, where L is the linear size of the system. We note here that the assumption of periodic boundary conditions is for simplicity. In principle, an Ewald summation procedure would be more accurate. The model construction is illustrated in Fig. 1. It is easy to see that in the limits $\gamma \rightarrow 0$ and $\gamma \rightarrow \infty$ we recover the two extreme cases of load redistribution in fiber bundle models: the global load sharing and the local load sharing, respectively. We should note here that, strictly speaking, for all γ different from the two limits above, the range of interaction covers the whole lattice. However, when changing this exponent, one moves from a very localized *effective* range of interaction to a truly global one as γ approaches zero. So, we will refer henceforth to a change in the *effective* range of interaction.

In summary, during an avalanche of failure events, an intact fiber i receives at each time step τ the load borne by failing elements j . Consequently, its load increases by an amount,

$$\sigma_i(t + \tau) = \sigma_i(t + \tau - 1) + \sum_{j \in B(\tau)} \sigma_j(t + \tau - 1)F(r_{ij}, \gamma), \quad (3)$$

where the sum runs over the set $B(\tau)$ of elements that have failed in a time step τ . Thus, $\sigma_i(t_0 + T) = \sum_{\tau=1}^T \sigma_i(t_0 + \tau)$ is the total load element i receives during an avalanche initiated at t_0 and which ended at $t_0 + T$. In this way, when an avalanche ends, the external field is applied again and another avalanche is initiated. The process is repeated until no intact elements remain in the system and the ultimate strength of the material σ_c , is defined as the maximum load the system can support before its complete breakdown.

Unfortunately, the complete analytical approach to the general model introduced here is inaccessible. There are a few cases where this task can be achieved such as the global load sharing model where the load acting on surviving elements for a given external force F is known [14,18] and some 1D models [30–32] (which are irrelevant for practical purposes). The main difficulty is that in order to analytically solve the problem, one needs to know the transition probabilities for all the possible paths leading the system from the state in which all the elements are intact to the state in which they have failed. This calculation eventually becomes impossible for large system sizes. So, a first step is to learn from Monte Carlo simulations which, furthermore, allows us to better understand the physical mechanisms of fracture and to study models difficult to handle analytically as well as to guide our search for analytical calculations.

III. MONTE CARLO SIMULATION OF THE FAILURE PROCESS

We have carried out large scale numerical simulations of the model described above in two dimensions. The fibers are identified with the sites of a square lattice of linear size L with periodic boundary conditions. The failure process is then simulated by varying the effective range of interaction between fibers by controlling γ , and recording the avalanche size distribution, the cluster size distribution and the ultimate strength of the material for several system sizes. Each numerical simulation was performed over at least 50 different realizations of the disorder distribution.

Figure 2 shows the ultimate strength of the material for different values of the parameter γ and several system sizes from $L = 33$ to $L = 257$. Clearly, two distinct regions can be distinguished. For small γ , σ_c is

independent, within statistical errors, of both the effective range of interaction and the system size. At a given point $\gamma = \gamma_c$ a crossover is observed, where γ_c falls in the vicinity of $\gamma = 2$. The region $\gamma > \gamma_c$ might eventually be further divided into two parts, the first region characterized by the dependence of the ultimate strength of the bundle on both the system size and the effective range of interaction; and a second region where σ_c only depends on the system size. This would mean that there might be two transition points in the model, for which the system displays qualitatively and quantitatively different behaviors. For $\gamma \leq \gamma_c$ the ultimate strength of the bundle behaves as in the limiting case of global load sharing, whereas for $\gamma \geq \gamma_c$ the local load sharing behavior seems to prevail. Nevertheless, the most important feature is that when decreasing the effective range of interaction in the thermodynamic limit, for $\gamma > \gamma_c$, the critical load is zero. This observation is further supported by Fig. 3, where we have plotted the evolution of σ_c as a function of $\frac{1}{\ln N}$ for different values of the exponent γ . Here, the two limiting cases are again clearly differentiated. For large γ all curves decrease when $N \rightarrow \infty$ as

$$\sigma_c(N) \sim \frac{\alpha}{\ln N} \quad (4)$$

This qualifies for a genuine short range behavior as found in LLS models where the same relation was obtained for the asymptotic strength of the bundle [19,20]. It is worth noting that in the model we are analyzing, the limiting case of local load sharing corresponds to models in which short range interactions are considered to affect the nearest and the next-nearest neighbors. In the transition region, the maximum load the system can support also decreases as we approach the thermodynamic limit, but in this case much slower than for $\gamma \gg \gamma_c$. It has been pointed out that for some modalities of stress transfer, which can be considered as intermediate between GLS and LLS, σ_c decreases for large system sizes following the relation $\sigma_c \sim \frac{1}{\ln(\ln N)}$ as in the case of hierarchical load transfer models [33]. In our case, we have fitted our results with this relation but we have not obtained a single collapsed curve because the slopes continuously vary until the LLS limit is reached. Finally, the region where the ultimate stress does not depend on the system size shows the behavior expected for the standard GLS model, where the critical load can be exactly computed as $\sigma_c = (\rho e)^{-1/\rho}$ for the Weibull distribution. The numerical values obtained for $\rho = 2$ are in good agreement with this later expression.

The fracture process can also be investigated by looking at the recursory activity before the complete breakdown. The statistical properties of rupture sequences are characterized by the avalanche size distribution which from the experimental point of view could be related to the acoustic emissions generated during the fracture of materials [34–37]. Figure 4 shows the avalanche size distribution for different values of γ . Again, we observe that for decreasing effective range of interaction (increasing γ)

there is a crossover in the distribution of avalanche sizes. The upper curves can be very well fitted by a power law $P(m) \sim m^{-\tau}$, with $\tau \approx \frac{5}{2}$, the value obtained for long range interactions [17–20].

As soon as the localized nature of the interaction becomes dominant $\gamma > \gamma_c$, the power law dependence of the avalanche size distribution with the exponent $\tau \approx \frac{5}{2}$ does not apply anymore. The lack of a characteristic size is a fingerprint of a highly fluctuating activity that could be related to the very nature of the long range interactions. The avalanche size distribution is a measure of causally connected broken sites and the spatial correlations in this limit are ruled out. All the intact elements have a nonzero chance to fail independently of the (spatial) rupture history, and any given element could be near to its rupture point regardless of its position in the lattice. This is not indeed the case when γ is large enough and the short range interaction prevails. Now, the spatial correlations are important and concentration of stress takes place in the fibers located at the perimeter of an already formed cluster. Fibers far away the clusters of broken elements have significantly lower stresses and thus the size of the largest avalanche is reduced as well as the number of failed fibers belonging to the same avalanche, leading to a lower precursory activity.

A further characterization of what is going on in the fracture process can be carried out by focusing on the properties of clusters of broken fibers. The clusters formed during the evolution of the fracture process are sets of spatially connected broken sites on the square lattice [6,12]. We consider the clusters just before the global failure and they are defined taking into account solely nearest neighbors connections. It is important to note that the case of global load sharing does not assume any spatial structure of fibers since it corresponds to the mean field approach. However, in our case it is obtained as a limiting case of a local load sharing model on a square lattice, which justifies the cluster analysis also for GLS. Fig. 5 illustrates how the cluster structure just before complete breakdown changes for various values of γ . We have also recorded the cluster size distribution as a function of the effective range of interaction. Figure 6 shows the size distribution $n(s_c)$, of the two-dimensional clusters for several values of the exponent of the load sharing function. The distributions have clearly two groups as found for other quantities also.

In the limit where the long range interaction dominates, the clusters are randomly distributed on the lattice indicating that there is no correlated crack growth in the system as well as that the stress is not concentrated in regions. The cluster structure of the limiting case of $\gamma = 0$ can be mapped to percolation clusters on a square lattice generated with the probability $0 < P(\sigma_c) < 1$, where σ_c is the fracture strength of the fiber bundle. However, the value of $P(\sigma_c)$ depends on the Weibull index ρ and is normally different from the critical percolation probability $p_c = 0.592746$ of the square lattice. Equality $P(\sigma_c) = p_c$ is obtained for $\rho = 1.1132$, hence, for

physically relevant ρ values used in simulations the system is below p_c at complete breakdown. This argument also justifies the exponential-like shape of the cluster size distributions of GLS in Fig. 6. This picture radically changes when the short range interaction prevails. In this case, the stress transfer is limited to a neighborhood of the failed elements and there appear regions where a few isolated cracks drive the rupture of the material by growth and coalescence. Thus, the probability of the existence of a weak region somewhere in the system is high and a weak region in the bundle may be responsible for the failure of the material. The differences in the structure of clusters also explain the lack of a critical strength when N goes to infinity in models with local rearrangement of stress. Since in the GLS model the clusters are randomly dispersed across the entire lattice, the system can “store” more damage or stress, whereas for LLS models a small increment of the external field may provoke a run away event ending with the macroscopic breakdown of the material.

Up to now, the change of the behavior of the system was observed for a certain value of γ analysing various measured quantities. All these numerical results suggest that the crossover between the two regimes occurs in the vicinity of $\gamma = 2$. Further support for the precise value of γ_c can be obtained by studying the change in the cluster structure of broken fibers. The moments of $n(s_c)$ defined as

$$m_k \equiv \int s_c^k n(s_c) ds \quad (5)$$

where m_k is the k th moment, describe much of the physics associated with the breakdown process. We will use these moments to quantitatively characterize the point where the crossover from mean field to short range behavior takes place. The zero moment $n_c = m_0$ is the total number of clusters in the system and is plotted in Fig. 7a as a function of the parameter γ . Figure 7b represents the variation of the total number of broken sites N_c (the first moment $N_c = m_1$) when γ increases. It turns out that up to a certain value of the effective range of interaction, N_c remains constant and then it decreases fast until a second plateau seems to arise. Note that the constant value of N_c for small γ is in agreement with the value of the fraction of broken fibers just before the breakdown of the material in mean field models. This property clearly indicates a change in the evolution of the failure process and may serve as a criterion to calculate the crossover point. However, a more abrupt change is observed in the average cluster size $\langle s_c \rangle$ at varying γ . According to the moments description, the average cluster size is equal to the second moment of the cluster distribution divided by the total number of broken sites, *i.e.* $\langle s_c \rangle = m_2/m_1$. It can be seen in Fig. 7d that $\langle s_c \rangle$ has a sharp maximum at $\gamma = 2.2 \pm 0.1$, and thus the average cluster size drastically changes at this point, which again suggests the crossover point to be in the vicinity of $\gamma_c = 2$.

We now discuss the finite size scaling (FSS) of the avalanche distributions. For local load sharing one expects that the cutoff in the avalanche distribution does not scale with L while for global load sharing the cutoff should scale with the size of the system. We have plotted in Fig. 8 the avalanche size distribution for several system sizes. As it can be observed, the FSS hypothesis is verified for the values of the exponent γ corresponding to the global (Fig. 8b) and the local (Fig. 8a) load sharing cases. Figure 8c shows the moment analysis for five different system sizes in the range $2.0 \leq \gamma \leq 2.5$. It can be seen that the position of the maximum of the m_2/m_1 curves is always at $\gamma = 2.2 \pm 0.1$, it does not scale with the system size. To determine the position of the crossover point more accurately we also analyzed the behaviour of α characterizing the strength of logarithmic size effect in Eq. (4), as a function of γ . From these studies it turned out that consistent interpretation of the numerical results can be given assuming that the crossover occurs in the vicinity of $\gamma_c = 2.0$ but stonger statement cannot be drawn due to the limited precision of calculations.

IV. DISCUSSION AND CONCLUSIONS

In the limiting case of global load sharing the breaking of fibers is a completely random nucleation process, there is no correlated crack growth in the system, and the fiber failure which results in the catastrophic avalanche occurs at a random position in the system. As long as this microscopic damage mechanism holds when changing the exponent γ , globally the system will behave in a global load sharing manner. On the other hand, when the load sharing is very localized, at the beginning of the failure process we get random nucleation of microcracks but later, correlated growth of clusters of broken fibers occurs. It then follows that along the perimeter of the clusters there is a high stress concentration and the final avalanche is driven by a fiber located at the perimeter of one of the clusters (the dominant one). At the fibers far away from the perimeter, the stress concentration is significantly lower, and the stress distribution is very inhomogeneous. In the case of localized load sharing this mechanism gives rise also to the logarithmic size effect as obtained also for the random fuse model [38].

An interesting aspect to be explored in future work is whether there is a second transition point in the model when the γ -dependence of σ_c seems to disappear or it is just a crossover. In the case of localized load sharing the global failure is caused, as noted before, by the instability of a cluster of broken fibers, defining a critical cluster size. Furthermore, the exact value of γ_c might depend on the amount of disorder in the system which will also be subject of future studies. Preliminary studies of this issue indicate that the transition value γ_c gets slightly smaller as the system becomes more homogeneous (increasing ρ).

Before setting our conclusions, we would like to remark that a similar transition to the one obtained here has been observed in other models. It is well-known that long range interactions between spins can affect the critical behavior of magnets. If we consider the addition of a term $\sum_{r,r'} V(r-r')s(r)s(r')$ to an Ising Hamiltonian, where $V(r) \sim r^{-(d+\sigma)}$ corresponds to a long range interaction decaying as a power law, a crossover to long range behavior is obtained provided that $\sigma < 2 - \eta_{sr}$, where η_{sr} is the value of the critical exponent η for short range force [39–41]. A similar behavior has also been reported in percolation phenomena with long range correlations [42].

In summary, we have studied a fracture model of the fiber bundle type where the interaction among fibers is considered to decay as a power law of the distance from an intact element to the rupture point. Two very different regimes are found as the exponent of the stress-transfer function varies and a crossover point is identified at $\gamma = \gamma_c$. The strength of the material for $\gamma < \gamma_c$ does not depend on both the system size and γ qualifying for mean-field behavior, whereas for the short range regime, the critical load vanishes in the thermodynamic limit. The behavior of the model at both sides of the crossover point was numerically studied by recording the avalanche and the cluster size distributions. The numerical results suggest that the crossover point falls in the vicinity of $\gamma_c = 2.0$. Finally, we have outlined some general ideas which will be the subject of a forthcoming publication.

V. ACKNOWLEDGMENTS

Y. M. thanks A. F. Pacheco and A. Vespignani for useful comments on the manuscript. This work began while one of the authors (Y. M.) was visiting the Institute for Computational Physics (ICA1) at the University of Stuttgart. Its financial support and hospitality are gratefully acknowledged. F. K. acknowledges financial support of the Bólyai János Fellowship of the Hungarian Academy of Sciences and of the Research Contract FKFP 0118/2001. This work was supported by the project SFB381, and by the NATO grant PST.CLG.977311.

-
- [1] *Statistical Models for the Fracture of Disordered Media*. Editors, H.J. Herrmann and S. Roux, North Holland (1990), and references therein.
 - [2] *Statistical Physics of Fracture and Breakdown in Disordered Systems*. B. K. Chakrabarti, L. G. Benguigui, Clarendon Press, Oxford (1997), and references therein.
 - [3] *Critical Phenomena in Natural Sciences*, D. Sornette, Springer-Verlag, Berlin (2000), and references therein.
 - [4] H. E. Daniels, *Proc. R. Soc. London A* **183**, 405 (1945).

[5] B.D. Coleman, *J. Appl. Phys.* **28**, 1058 (1957); *ibid* **28**, 1065 (1957).

[6] S. Zapperi, P. Ray, H. E. Stanley, A. Vespignani, *Phys. Rev. Lett.* **78**, 1408 (1997).

[7] Y. Moreno, J. B. Gómez, A. F. Pacheco, *Phys. Rev. Lett.* **85**, 2865 (2000).

[8] S.L. Phoenix and L. Tierney, *Eng. Fracture Mech.* **18**, 193 (1983).

[9] W.I. Newman, A.M. Gabrielov, T.A. Durand, S.L. Phoenix and D.L. Turcotte, *Physica D* **77**, 200 (1994).

[10] W.I. Newman, D.L. Turcotte and A.M. Gabrielov, *Phys. Rev. E* **52**, 4827 (1995).

[11] M. Vázquez-Prada, J. B. Gómez, Y. Moreno, A. F. Pacheco, *Phys. Rev. E* **60**, 2581 (1999).

[12] F. Kun, S. Zapperi, H. J. Herrmann, *Eur. Phys. J.* **B17**, 269 (2000).

[13] D. Sornette, *J. Phys. A* **22**, L243 (1989).

[14] D. Sornette, *J. Phys. I France* **2**, 2089 (1992).

[15] W. A. Curtin, *Phys. Rev. Lett.* **80**, 1445 (1998).

[16] S. Mahesh, I. J. Beyerlein, S. L. Phoenix, *Physica D* **133**, 371 (1999).

[17] A. Hansen, P. C. Hemmer, *Phys. Lett. A* **184**, 394 (1994).

[18] P. C. Hemmer, A. Hansen, *J. Appl. Mech.* **59**, 909 (1992).

[19] D. G. Harlow, *Proc. R. Soc. London A* **397**, 211 (1985).

[20] M. Kloster, A. Hansen, P. C. Hemmer, *Phys. Rev. E* **56**, 2615 (1997).

[21] D. L. Turcotte, *Fractals and Chaos in Geology and Geophysics*, 2nd Edition, Cambridge University Press, Cambridge, New York (1997).

[22] C. Moukarzel, P. M. Duxbury, *J. Appl. Phys.* **76**, 1(1994).

[23] D. G. Harlow, S. L. Phoenix, *J. Composite Mater.* **12**, 195 (1978).

[24] R. L. Smith, S. L. Phoenix, *J. Appl. Mech.* **48**, 75 (1981).

[25] C. Baxenvanakis, D. Jeulin, J. Renar, *Int. J. Fract.* **73**, 149 (1995).

[26] I. J. Beyerlein, S. L. Phoenix, *Eng. Fract. Mech.* **57**, 241 (1997).

[27] I. J. Beyerlein, S. L. Phoenix, *Eng. Fract. Mech.* **57**, 267 (1997).

[28] M. Ibnabdeljalil, W. A. Curtin, *Int. J. Solids Structures* **34**, 2649 (1997).

[29] M. Ibnabdeljalil, W. A. Curtin, *Acta Mater.* **45**, 3641 (1997).

[30] B. Q. Wu, P. L. Leath, *Phys. Rev. B* **61**, 15028 (2000).

[31] B. Q. Wu, P. L. Leath, *Phys. Rev. B* **59**, 4002 (1999).

[32] S. L. Phoenix, I. J. Beyerlein, *Phys. Rev. E* **62**, 1622 (2000).

[33] W. I. Newman, A. M. Gabrielov, *Int. J. Fract.* **50**, 1 (1991).

[34] A. Garcimartin, A. Guarino, L. Bellon, S. Ciliberto, *Phys. Rev. Lett.* **79**, 3202 (1997).

[35] A. Guarino, A. Garcimartin, S. Ciliberto, *Eur. Phys. J. B* **6**, 13 (1998).

[36] C. Maes, A. van Moffaert, H. Frederix, H. Strauven, *Phys. Rev. B* **57**, 4987 (1998).

[37] A. Petri, G. Paparo, A. Vespignani, A. Alippi, M. Costantini, *Phys. Rev. Lett.* **73**, 3423 (1994).

[38] B. Kahng, G. G. Bartrouni, S. Redner, L. de Arcangelis and H. J. Herrmann *Phys. Rev. B* **37**, 7625 (1988).

[39] J. Cardy, *Scaling and Renormalization in Statistical*

Physics, Cambridge Lectures Notes in Physics 5, Cambridge University Press, Cambridge (1996).

[40] J. Sak, *Phys. Rev. B* **15**, 4344 (1977).

[41] E. Brézin, J. Zinn-Justin, J. C. Le Guillou, *J. Phys. A: Math. Gen.* **9**, L119 (1976).

[42] M. Sahimi, *Phys. Rep.* **306**, 213 (1998).

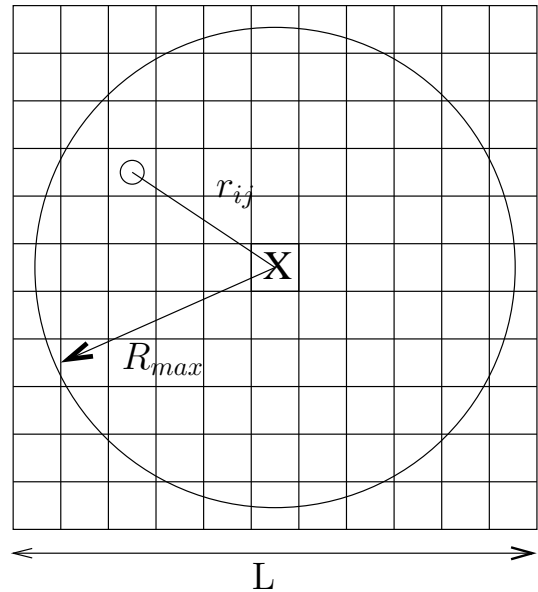


FIG. 1. Illustration of the model construction. \times indicates a fiber, which is going to break, and \circ is an intact fiber in the square lattice.

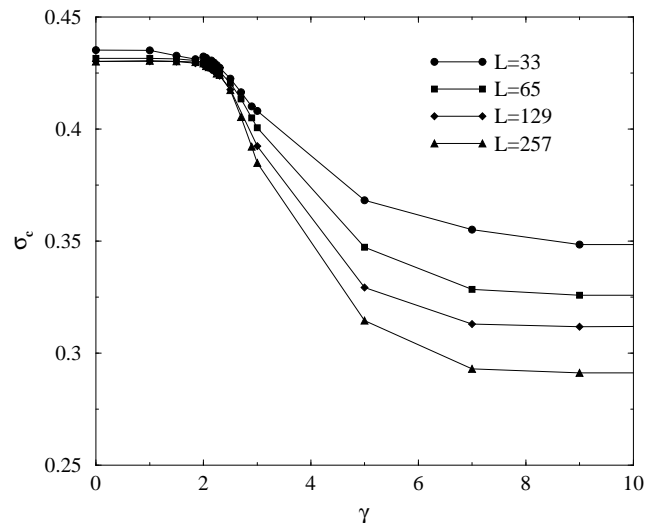


FIG. 2. Ultimate strength of the material for different system sizes as a function of the effective range of interaction γ . A crossover from mean field to short range behavior is clearly observed.

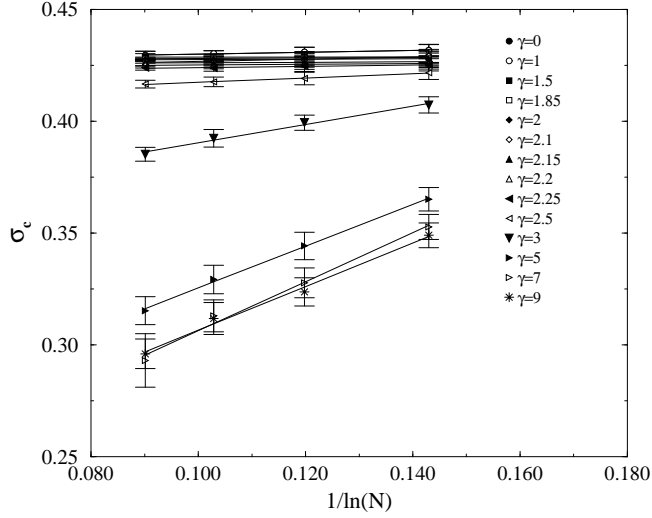


FIG. 3. Variation of the material strength with N for several values of γ . Note that when γ increases the critical load vanishes in the thermodynamic limit, whereas, for small γ it has a nonzero value independent on the system size.

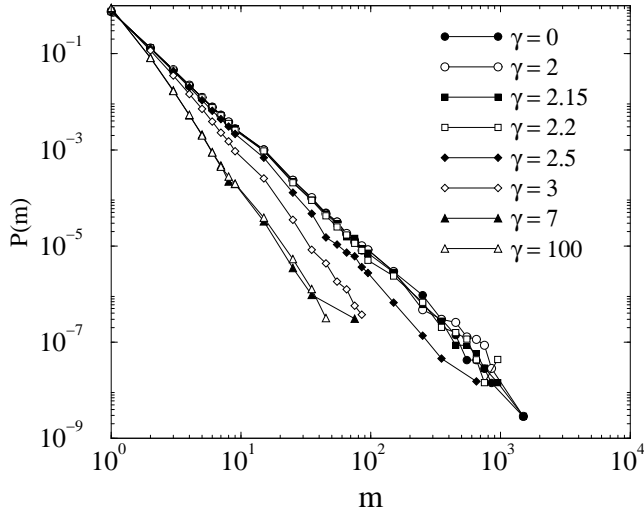


FIG. 4. Avalanche size distributions for different values of the exponent of the stress-transfer function γ . The upper group of curves can be very well fitted with a straight line with a slope $\tau = -\frac{5}{2}$ ($L = 257$).

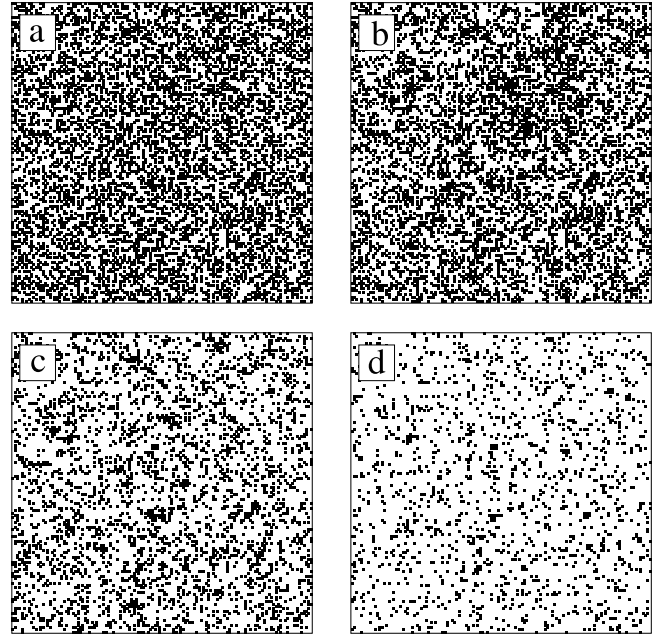


FIG. 5. Snapshots of the clusters just before the complete breakdown of the material. The change in the structure of the clusters can be seen. The values of γ are: a) $\gamma = 0$, b) $\gamma_c = 2.2$, c) $\gamma = 3$, and d) $\gamma = 9$.

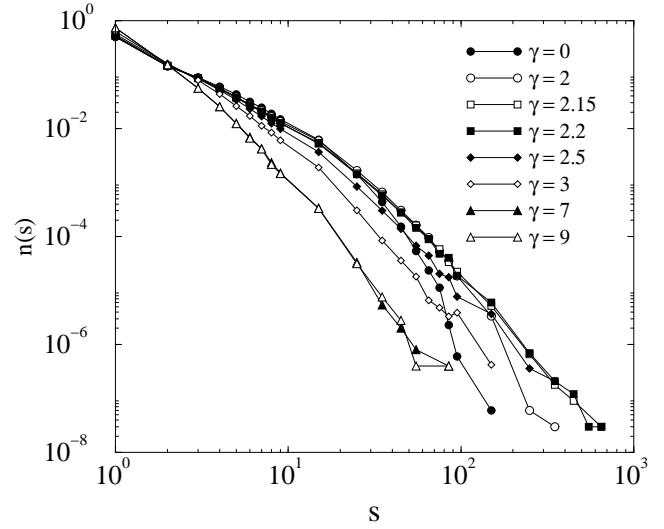


FIG. 6. Cluster size distributions for different values of the stress-transfer function exponent γ . Clearly, two different groups of curves can be distinguished as found for other quantities also ($L = 257$).

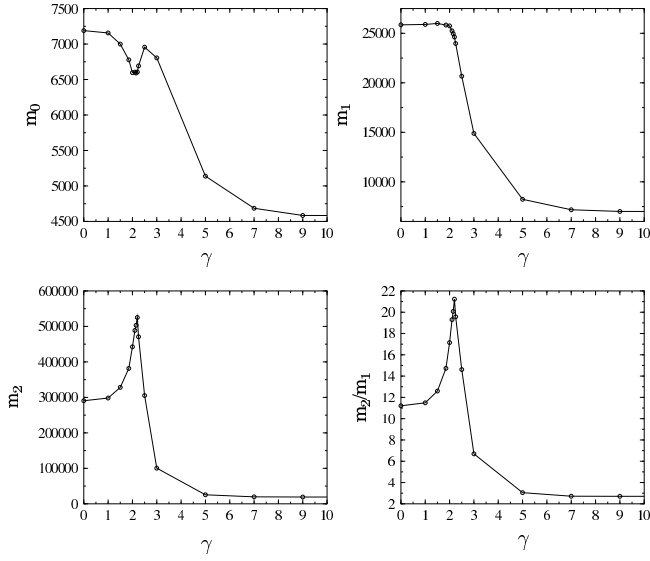


FIG. 7. Moments of the cluster size distribution as a function of γ (see text for details on the definition of m_k). A sharp maximum is observed at $\gamma = \gamma_c \sim 2.2$ for the average cluster size $\langle s_c \rangle = \frac{m_2}{m_1}$.

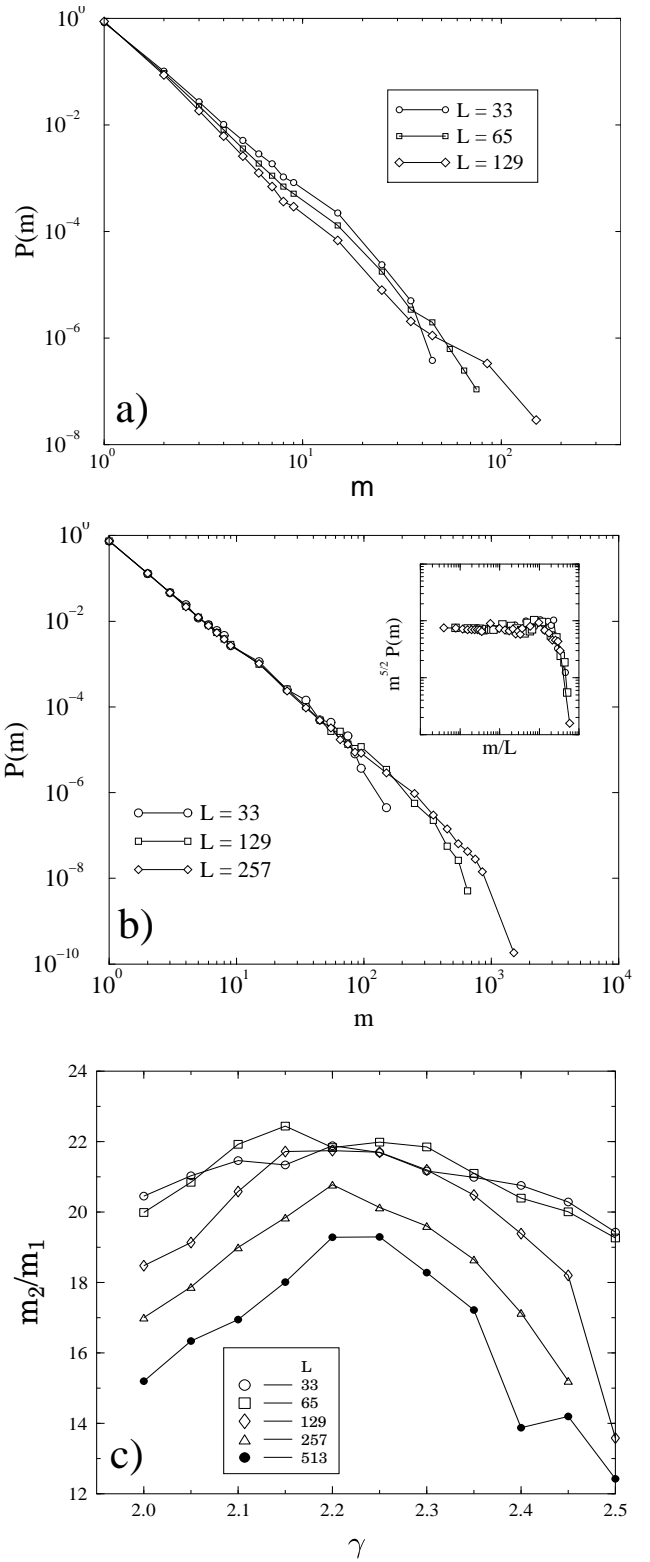


FIG. 8. Finite size scaling analysis. *a*) Scaling of the cutoff with the system size for the local load sharing case, *b*) Scaling of the cutoff with the system size for the global load sharing case, and *c*) Average cluster size, $\langle s_c \rangle = \frac{m_2}{m_1}$, for different system sizes. Note that in *c*) the position of γ_c does not change.